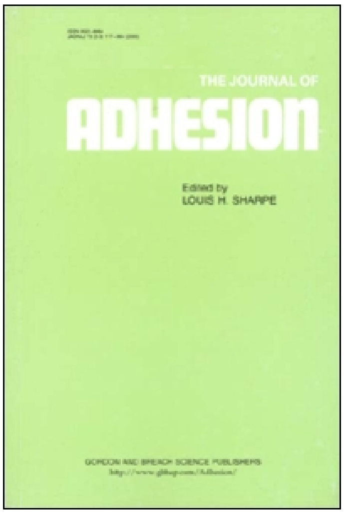

The Journal of Adhesion
Publication details, including instructions for authors and subscription information:
http://www.informaworld.com/smpp/title~content=t713453635

Bi-Material Joining for Car Body Structures: Experimental and Numerical Analysis

M. Avalle[a]; L. Peroni[a]; M. Peroni[a]; A. Scattina[a]
[a] Politecnico di Torino, Torino, Italy

Online publication date: 10 June 2010

To cite this Article Avalle, M. , Peroni, L. , Peroni, M. and Scattina, A.(2010) 'Bi-Material Joining for Car Body Structures: Experimental and Numerical Analysis', The Journal of Adhesion, 86: 5, 539 — 560
To link to this Article: DOI: 10.1080/00218464.2010.484308
URL: http://dx.doi.org/10.1080/00218464.2010.484308

The Journal of Adhesion, 86:539–560, 2010

ISSN: 0021-8464 print/1545-5823 online
DOI: 10.1080/00218464.2010.484308

Bi-Material Joining for Car Body Structures: Experimental and Numerical Analysis

M. Avalle, L. Peroni, M. Peroni, and A. Scattina
Politecnico di Torino, Torino, Italy

Crashworthiness is an important issue in car body design: it describes the ability of the vehicle structure to behave efficiently by absorbing and dissipating energy in a stable and controlled manner during a crash event. Energy management during frontal impact is mainly done through crash boxes in the front rails. These crash boxes are usually slender, thin-walled steel columns, progressively collapsing during impact. Due to a trend in lightweight materials use, it is necessary to gain knowledge about the material behaviour and alternative joining systems. The use of an adhesive as a joining system for different materials was investigated by means of experimental tests on specimens and simple components, made of aluminium and deep drawing steel. A numerical simulation technique was developed to describe and understand the phenomenon. Furthermore, since the behaviour is influenced by the loading rate and the materials used in this application are known to be strain-rate sensitive, static and impact loading conditions were examined.

Keywords: Car body structures; Crash boxes; Energy absorbing components

1. INTRODUCTION

A very important issue in car design nowadays is the trend in using new, smart, and multifunctional materials. In the near future, well-known and widely used materials like deep-drawing steels will be progressively substituted by high strength steels, aluminium alloys, magnesium alloys, and various types of polymeric materials and composites [1,2]. There are several reasons for this change: the structure weight reduction, the need for higher stiffness and strength of the

Received 22 June 2009; in final form 13 October 2009.
Presented in part at the 3rd International Conference on Advanced Computational Engineering and Experimenting (ACE-X 2009), Rome, Italy, 22–23 June 2009.
Address correspondence to Massimiliano Avalle, Politecnico di Torino, Corso Duca degli Abruzzi 24, 10129 Torino, Italy. E-mail: massimiliano.avalle@polito.it

car body structure and last, but not least, cost reduction. Many problems are linked to the introduction of new materials: their properties are still not completely known, the usually adopted technologies are sometimes not usable anymore, and new environmental and protection problems arise. Additional problems are associated with the joining techniques. For several years, car body assembly techniques were fully dominated by spot-welding, but resistance spot-welding cannot be used to join different materials. The same (SW) is true for other welding techniques for metals, such as, for example, laser welding (LW).

Among the various alternative solutions that include mechanical joining by means of screws, rivets, self-piercing connections, clinch joints, etc., the most promising are structural adhesives. The use of structural adhesives in car body construction has a lot of advantages: the joint is not localized in small areas (thus, stress concentrations are nearly eliminated); the adhesive layer produces additional insulation, protection, and damping; and, finally, it is possible to join different materials of almost any kind. The main drawbacks in using adhesives are the residual stresses in the adhesive layer that derive from the differences in the coefficient of thermal expansion of the adherends and of the adhesive itself, and their relatively low peel strength. However, state-of-the-art structural adhesives have reached very good peel strength, largely sufficient to guarantee very effective joint strength. Many other supposed drawbacks can be worked around by using state-of-the-art knowledge on adhesive joint construction. Surface preparation is little nowadays nor necessary anymore: modern structural adhesives can be applied directly on untreated surfaces, even dirty and greasy surfaces [3]. The long curing time can still pose some problems, but, by using bonded joints together with other mechanical fastening techniques, or with temporary fasteners [4], this problem can be effectively solved: the usual oven treatment for car body paints is then exploited for adhesive polymerisation, too, if necessary. Probably the main concern in using adhesives, as for many polymer materials, relates to long-term endurance, which is still not completely known, especially in severe environments. However, this problem is also quite overestimated: the adhesive layer is practically isolated from environmental detrimental agents, like light rays (except for the occasional case of transparent adherends), water, oxygen, and chemicals.

On the whole, the major problem lies in incorrect design of the adhesive joint. A correctly designed and realized bonded joint is as reliable as other joining systems.

This work aims to contribute to the knowledge of adhesive bonding systems for crashworthy applications. Several works have been published on this topic in recent years [3–12]. However, very little is known about joining of dissimilar materials and of their crash behaviour.

To this objective, simple thin-walled, square section columns made of two joined parts were subjected to axial crushing comparing the behaviour of different material combinations. Joining of two thin-walled half columns, previously obtained by deep drawing, is the usual way to build components like crash boxes for the front of cars: they are usually made of some low carbon steel and joined by SW. In this work, steel/steel, aluminium/aluminium, and aluminium/steel combinations were examined. Two kinds of sections have been examined: the classical top-hat section and a closed double-C section. In view of the application studied, the effect of loading speed was also examined. Finally, a numerical model was developed: simulation of the kinds of situations is necessary for the design of vehicle structures that can be subjected to impact and crash. The model was restricted to quasi-static loading because the interest was focused on finding the right practices to reproduce the phenomenon, without entering into full details such as strain-rate modelling of the materials that is an established method today.

The results were analysed mainly in terms of specific absorbed energy, and it is shown that adhesives are a very efficient solution for joining dissimilar materials, and can also improve efficiency compared with the basic solution.

2. ENERGY ABSORPTION

Crash boxes are the main energy management devices acting during a frontal crash. They are usually made of a thin-walled section obtained by joining two half columns. Energy absorption and dissipation occurs mainly from the process of progressive axial collapse through plastic folding [13–25]. During this process, energy is absorbed through plastic work. The specific absorbed energy, P_m, is the amount of plastic work divided by the crushing length (Fig. 1):

$$P_m = \frac{\int_0^L P(x)dx}{L}, \tag{1}$$

where $P(x)$ is the crushing load as a function of the actual crushing distance, x; L is the total crushing length. P_{m} is then the average value of the crushing load, and it is the best estimator of the crashworthiness performance. The average crushing load depends on many

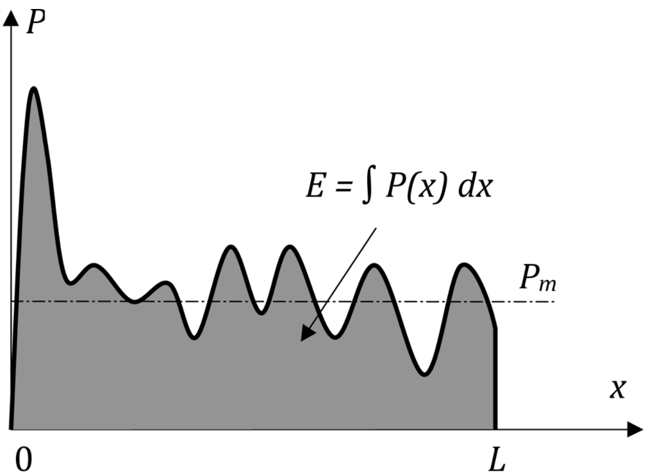

FIGURE 1 Energy absorption diagram during a typical crushing process by plastic progressive collapse.

influencing factors that can be synthetically represented by the following relation for a rectangular section [12]:

$$P_m = k\sigma_y^n a^p \left(\frac{b}{a}\right)^q t^r f^s, \tag{2}$$

where a and b are the sides of the rectangular section, t the shell thickness, f the flange width, and σ_y the yield strength of the material. The constants in Eq. (2) were found in several published papers [12–25].

When dealing with these and other innovative materials, joining is an important and challenging issue, especially when dealing with hybrid structures made of different materials. For continuous joining techniques, interesting and fundamental work was presented by Fay and Suthurst [5]. In this work, the effect of section design on the impact performance of bonded box beam sections was discussed and the results of tests carried out on redesigned sections were presented. Their work showed that simple substitution of spot-welding with bonding or weld-bonding in the same geometrical solution for the parts to be assembled was not satisfactory. They limited the analysis to a single material for both parts. Rivett *et al.* came to a similar conclusion [7]. Also, Avalle *et al.* [6] performed impact testing on bonded beams: they showed that the axial crush behaviour of crash boxes assembled by bonding is quite good, provided that the shape of the cross section and of the joint does not induce peeling in it, confirming somewhat the

Fay and Suthurst results. Since then, however, very tough, crash-resistant adhesives have been developed and great improvement can be obtained. As shown, for example, in [3], these new adhesives, with very high peeling strength, can improve energy absorption even in unfavourable loading conditions.

3. TEST CAMPAIGN SPECIFICATIONS

3.1. Specimen

The analysis of the ability of adhesives in joining similar and dissimilar materials for crash applications was performed by loading a series of crash boxes as shown in Fig. 2. They were constructed by assembling two thin-walled half shells. The first configuration, Fig. 2a, is the classical top-hat section found in most industrial solutions: it is made of a plate and of an omega section. This solution is very convenient

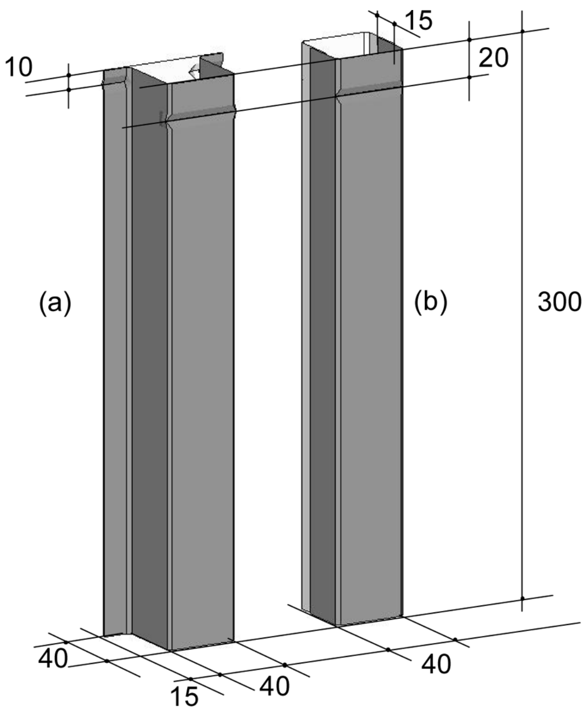

FIGURE 2 Schematic drawings of the crash boxes used in the current study: (a) top-hat section; (b) double-C section. The total length, the square size of the enclosed section, and the width of the flanges are the same for all examined configurations (dimensions in mm).

for SW but is also interesting for bonding since it allows for clamping the two parts together during polymerization of the adhesive. The second configuration, Fig. 2b, is a double-C section obtained by joining two identical C section parts with a partial overlap. This configuration, admissible with bonding, is more favourable when dealing with adhesives since the joint is loaded mainly in shear mode and not in peeling mode which is critical for the adhesive joint itself.

The decision on the dimensions to allow for comparison is not a straightforward process. If the enclosed square section ($40 \times 40\,mm$) is maintained, the total amount of material varies from one section to the other. The simple double-C square section, Fig. 2b, is lighter than the top-hat, Fig. 2a, if the overlap area is maintained constant. The following solution was then chosen, to maintain the width of the flanges in the top-hat section equal to the overlap area (that is, two times $300 \times 15\,mm$, that gives a total of $9000\,mm^2$).

A recurrent problem in laboratory axial crash tests on a simple column relates to the initiation of collapse. If a straight column is compressed between two rigid flat parallel plates, a first higher peak load occurs: this very high peak can induce global instability and it is often the cause of irregular folding and other problems (vibrations, measurement difficulties, premature failure by separation of the sheets, etc.). To avoid this, both in laboratory tests and in real applications, collapse initiators or triggers are built near the impacted end of the column. Collapse initiators can be of several types: holes [12], punch, bellows, etc. In the current work, collapse initiators were obtained by a small indentation at the prescribed position. The optimal position for the trigger is at the half of the basic folding length. The folding length must be estimated on the basis of past experiences or based on calculations [18,19,21,22]. The indentation was obtained by means of a controlled small fold of the end of the columns in a die (Fig. 3). This method, although quite simple, was found very effective.

3.2. Materials of the Adherends

Two materials were used in the work:

- A low-carbon deep-drawing steel (DC02 EN10130) which is still mostly used in many vehicle structures, and
- A medium strength aluminium alloy (1200-H14) which is an interesting substitution for steel in many applications.

The basic material data, from tests made internally, for both steel and aluminium are reported in Table 1.

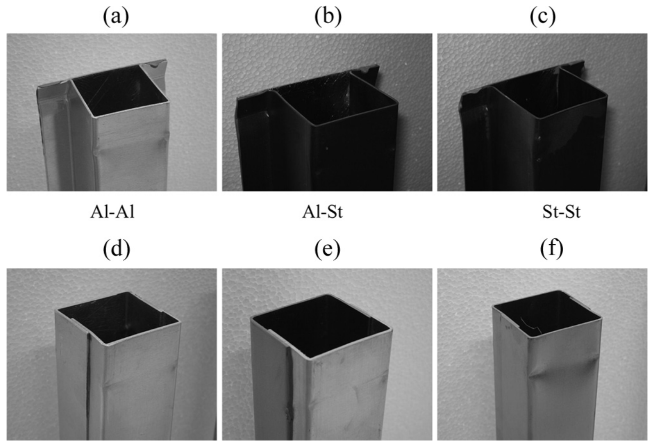

FIGURE 3 Top-hat and double-C column ends showing the collapse initiators.

Although the interest in the automotive industry is in using more and more high-strength low-alloy steel, DC0x sheet steel is still widely used, being easily worked and relatively cheap. Moreover, a large amount of data, both on the material and on joining of the same material, is available and that allows for comparisons and in-depth analysis. 1200 is a widespread aluminium alloy, preferable in terms of material cost to other series alloys widely used for sheet metal applications.

3.3. Adhesives

In the past, several studies were done with structural adhesives designed for automotive applications in car body components [11,12,26–29]. These adhesives are mainly epoxy resins, sometimes heat cured. Among the most interesting for crash applications is

TABLE 1 Basic Material Properties

Material	Steel, DC02 EN10130	Aluminium, 1200-H14
Elastic modulus, E (MPa)	200×10^3	70×10^3
Yield strength, σ_y (MPa)	170–280	115–120
Ultimate tensile strength, σ_u (MPa)	270–400	125–130
Elongation at failure, ε_u (%)	25–30	10–15
Power law constant, K (Mpa)	514	151
Power law exponent, n	0.172	0.0354

Loctite® Hysol® 9514. It is an interesting high performance structural adhesive, giving an average shear strength measured according to ASTM D1002-94 of more than 50 MPa on steel [12], and a peel strength according to ASTM D1876-95 of 190-230 N/mm [12], also on steel. The maximum operative temperature limit is quite high for an adhesive: strength reduction becomes important only above 120°C. Moreover, Loctite Hysol 9514 has great toughness which is important in impact situations, much greater than similar adhesives such as Loctite Hysol 9466 [12]. Strength and energy absorption is three to four times as high. Table 2 summarizes some of the main material properties for this adhesive.

3.4. Experimental Setup

The tests consisted of the deep axial compression of the above-described thin-walled columns between two rigid flat and parallel plates, measuring the collapse load and stroke during the tests. The tests were conducted at low speed, in quasi-static loading conditions (0.5 mm/s), and at high speed (impact velocity $v_{inp} = 6$ m/s), by impact of a large mass with a prescribed initial velocity and energy.

Two types of equipment were used. For the lower range of speed a hydraulic universal material testing machine (DARTEC HA100, with 100 kN maximum load and 100 mm/s maximum speed Zwick, Ulm, Germany) was used. The machine is controlled by an electronic unit (DARTEC 9600 Stourbridge, UK) that also performs the data acquisition. Acquired data are the samples of the compression load and of the stroke. Load was measured by a 100 kN strain-gage load cell, whereas the stroke was measured by means of a 100 mm LVDT displacement transducer mounted on the hydraulic actuator.

The impact tests were performed by a specially built apparatus (ComPULSE) moved by a pneumatic actuator (Fig. 4). The actuator,on

TABLE 2 Basic Adhesive Properties (Data not Coming from [12] are from the Manufacturer's Technical Data Sheet)

Material	Loctite® Hysol® 9514
Bulk modulus (ASTM D882, GPa)	1.46
Elongation (ASTM D882, %)	5.8
Tensile strength (ASTM D882, Mpa)	44
Average shear strength (ASTM D1002-94, MPa) [12]	50 (steel)
Average shear strength (ASTM D1002-94, MPa)	40 (aluminium)
Peel strength (ASTM D1876-95, kN/mm) [12]	190–230 (steel)
Density (kg/dm^3)	1.44
Glass transition temperature (ASTM E1640-99, °C)	133

top in the figure, is filled with compressed air with the piston blocked. At the requested pressure, the piston is suddenly released and accelerated by the internal pressure. This way, in a very limited space, high speed values, up to 15 m/s, are obtained with sufficient energy to compress typical energy absorption components (maximum energy is approximately 5 kJ). Load is then measured with a piezoelectric 120 kN Kistler 9371B load cell (Kistler, Winterthur, Switzerland), the displacement is measured by a high speed triangulation laser transducer (Keyence LK-G407, Keyence, Osaka, Japan). Data are recorded with a National Instruments 6132, 3 MS/s, 14 bit, data acquisition card (National Instruments, Austin, TX, USA) and a LabView® program.

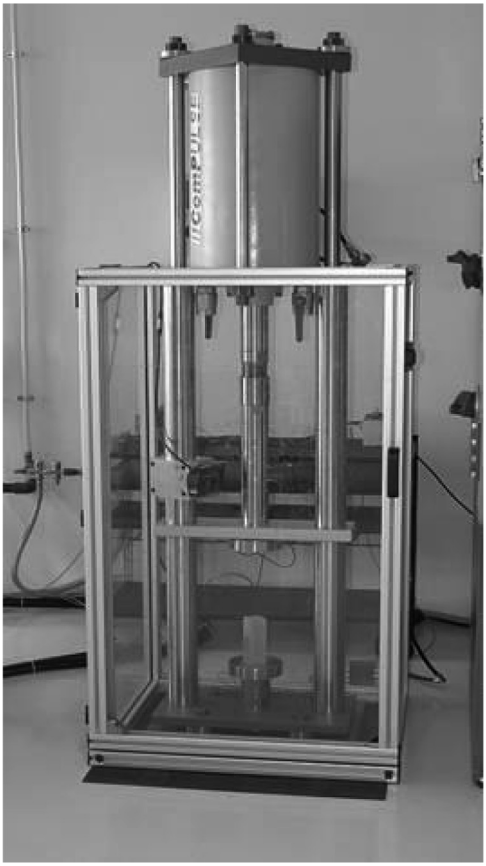

FIGURE 4 The ComPULSE equipment for compression testing.

4. EXPERIMENTAL TESTS

The following paragraph reports the results from the crushing tests on the described bonded columns. Even if several repetitions of the same configuration were done, the charts are plotted with two curves only for the sake of clarity.

4.1. Top-Hat Section

Figure 5 shows the results from quasi-static tests performed on the top-hat columns, in terms of the load-stroke curves. The behaviour of these components follows the classical pattern with a first peak higher than the following repeated at each fold formation. Moreover, for each fold there are two peaks, one smaller than the other: this corresponds to the two phases of fold formation—first outwards then inwards (the fold formation is clearly visible in the sequences of Fig. 6, excluding the third row for which the specimen shows defective fold formation). It is clear that after the formation of the first fold, with its associated first peak, the load-curve remains stable because of the stable and progressive formation of the successive folds. This observation is confirmed by the images taken during the plastic progressive collapse (Fig. 6) at various times. For the case of the hybrid structures, steel with aluminium, there are two possibilities: the hat can be made of steel or aluminium, and vice versa for the plate. The case of the aluminium hat joined to the steel plate brings unstable solutions: as shown in Fig. 6, third row, there is debonding causing reduced energy

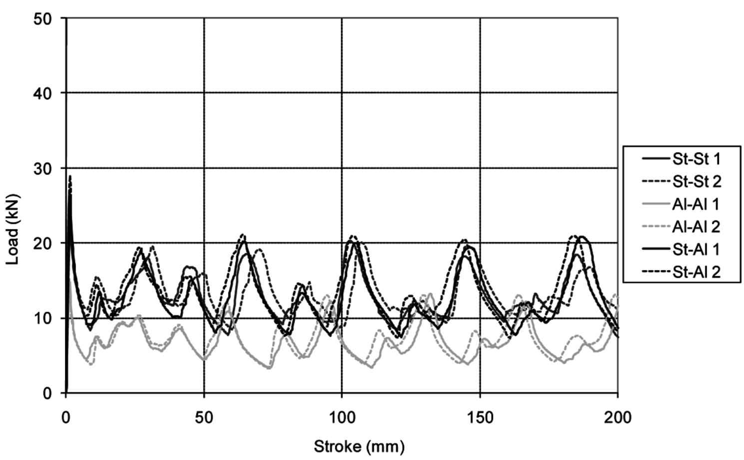

FIGURE 5 Load-stroke curves obtained from the top-hat section columns in quasi-static conditions (0.5 mm/s).

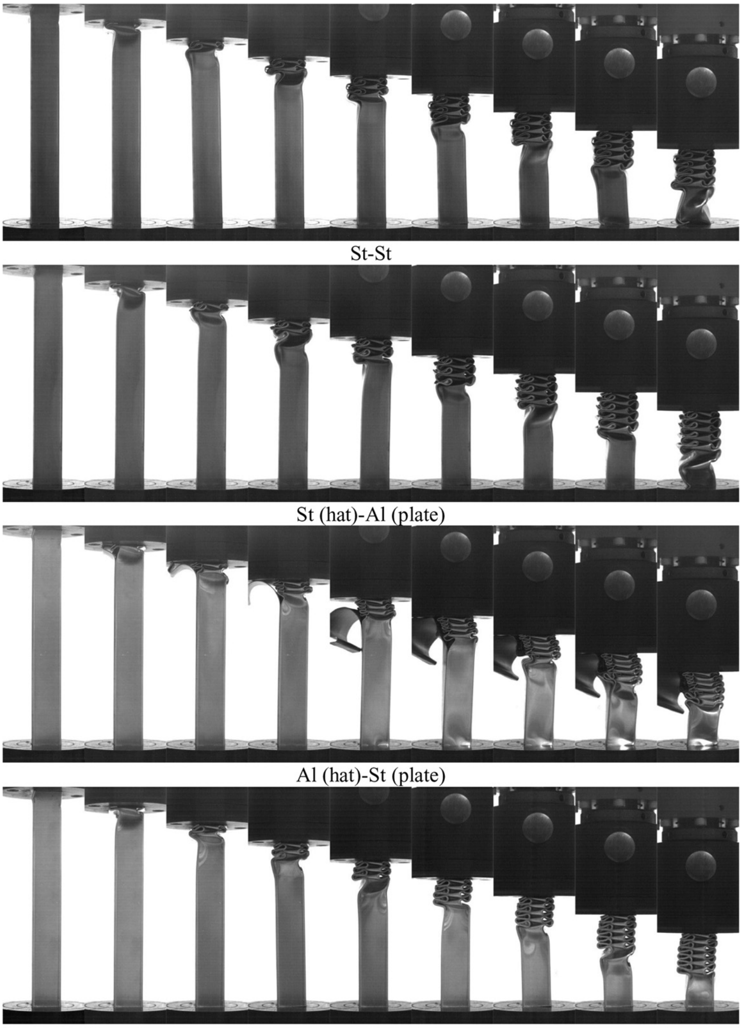

FIGURE 6 Progressive collapse of the top-hat section columns under quasi-static loading.

dissipation (this result was not reported in the chart of Fig. 5). On the contrary, the steel hat joined to the aluminium plate improves the collapse stability: even more, it brings more energy dissipation than in the case of steel bonded to steel (this will be discussed later).

A similar result holds for dynamic impact loading (Fig. 7). The average mean load is more or less comparable for the two cases of steel

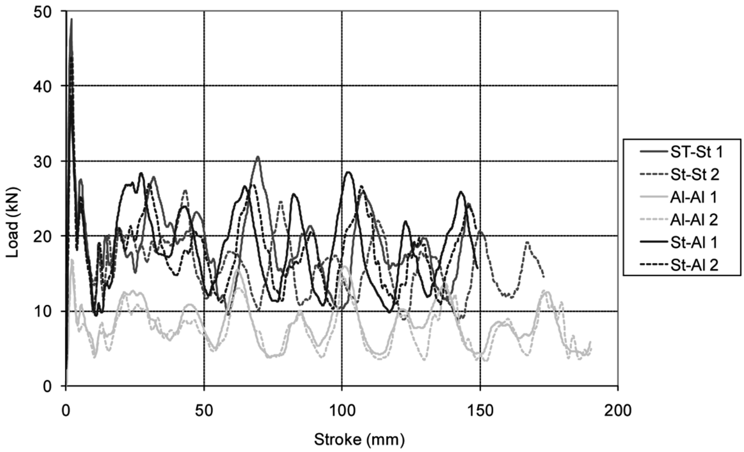

FIGURE 7 Load-stroke curves obtained from the top-hat section columns in dynamic conditions ($v_{imp} = 6\,\mathrm{m/s}$).

hat joined to steel plate, and steel hat joined to aluminium plate. Again, the case of an aluminium hat joined to a steel plate gives a more unstable collapse and much less energy absorption. However, there is some difference from the quasi-static case: the dynamic loading tends to stabilize the collapse because of transverse inertia force, as is well known [12–19,21–25], and some more energy dissipation is obtained, at least during the formation of the first folds (Fig. 8). Afterwards, the column tends to bend and to lose its capacity of maintaining the collapse load.

4.2. Double-C Section

For this solution, there are no options when joining steel to aluminium, since the section is symmetrical. The results from the quasi-static tests are reported in Fig. 9 in terms of load-stroke curves. Here again, the repeated load pattern is maintained quite regularly in all the cases. Despite the lack of symmetry of the hybrid steel with aluminium solution, the collapse remains stable as for the cases with similar parts (Fig. 10). On the whole, the hybrid solution shows an intermediate behaviour in terms of energy absorption.

Similar mechanical behaviour, almost unexpectedly, was obtained under dynamic loading (Fig. 11 and 12). The collapse remains stable and the energy absorption of the hybrid solution is intermediate between steel only and aluminium only columns.

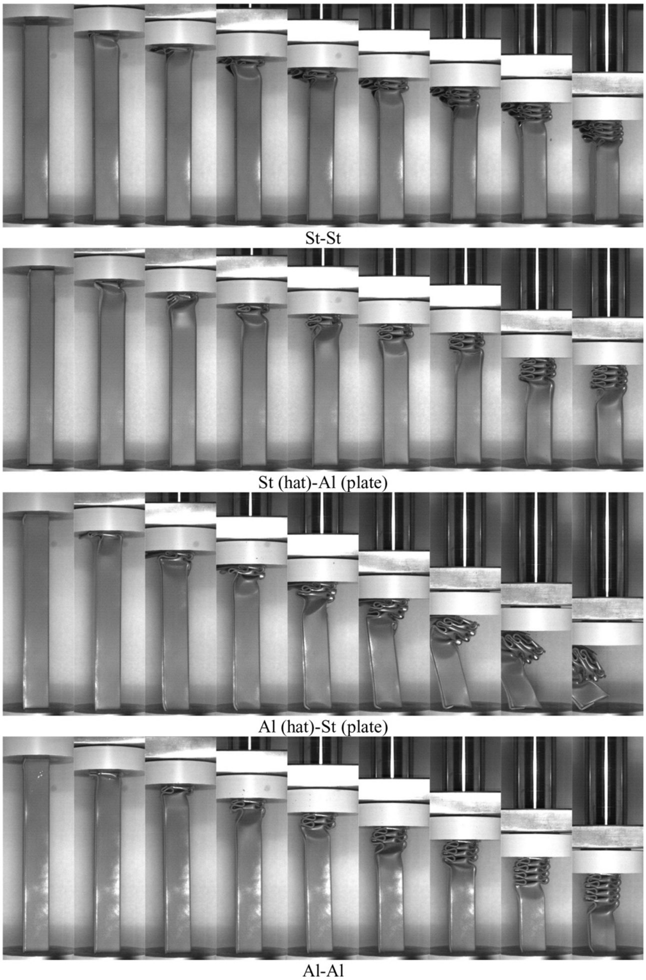

FIGURE 8 Progressive collapse of the top-hat section columns under dynamic loading.

4.3. Comparison of the Experimental Results

A comparison can be made in terms of average collapse load, P_m, as an indicator of the average absorbed energy. This is justified by observation of the energy absorption diagrams, which show the absorbed energy as a function of the displacement, that have a markedly linear trend (Fig. 13).

The hybrid solution is, apparently, only interesting in the case of the top-hat section. In this case, when a steel hat is joined to an

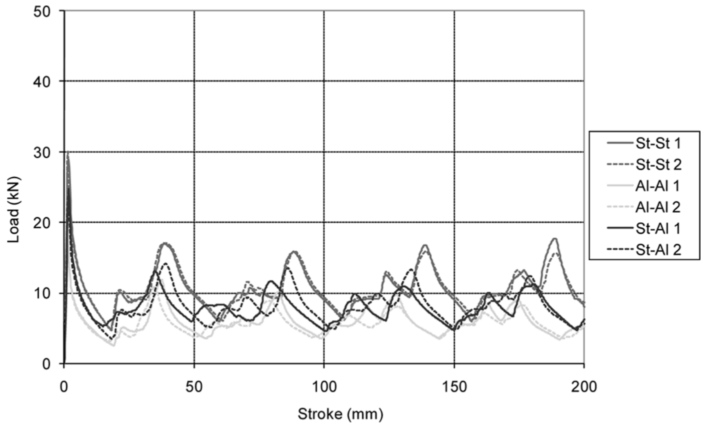

FIGURE 9 Load-stroke curves obtained from the double-C section columns in quasi-static conditions (0.5 mm/s).

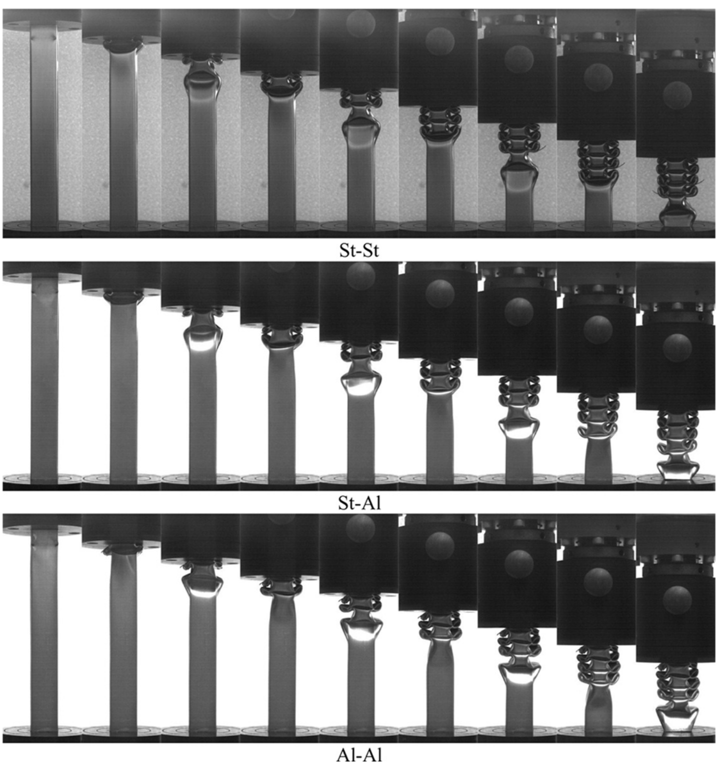

FIGURE 10 Progressive collapse of the double-C section columns under quasi-static loading.

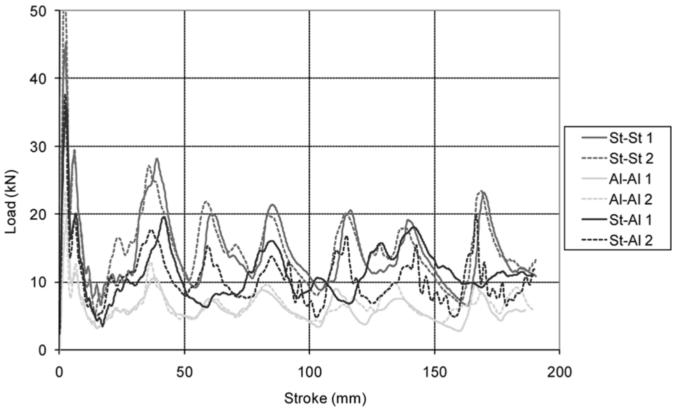

FIGURE 11 Load-stroke curves obtained from the double-C section columns in dynamic conditions ($v_{imp} = 6\,\mathrm{m/s}$).

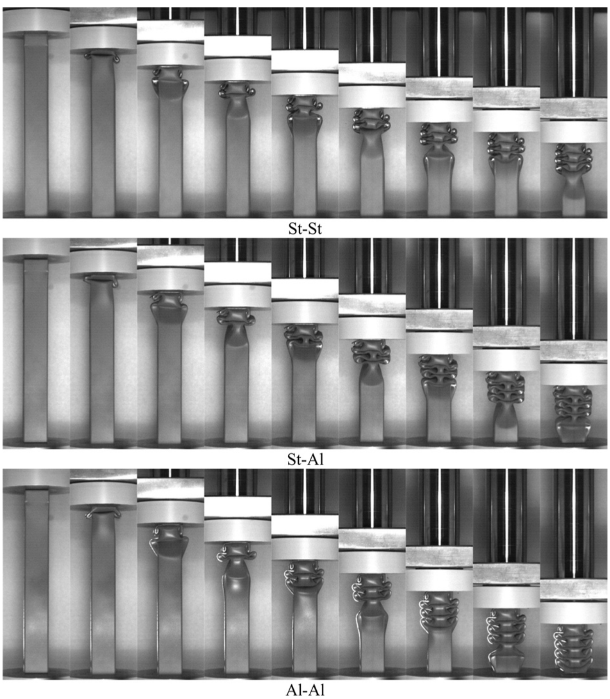

FIGURE 12 Progressive collapse of the double-C section columns under dynamic loading.

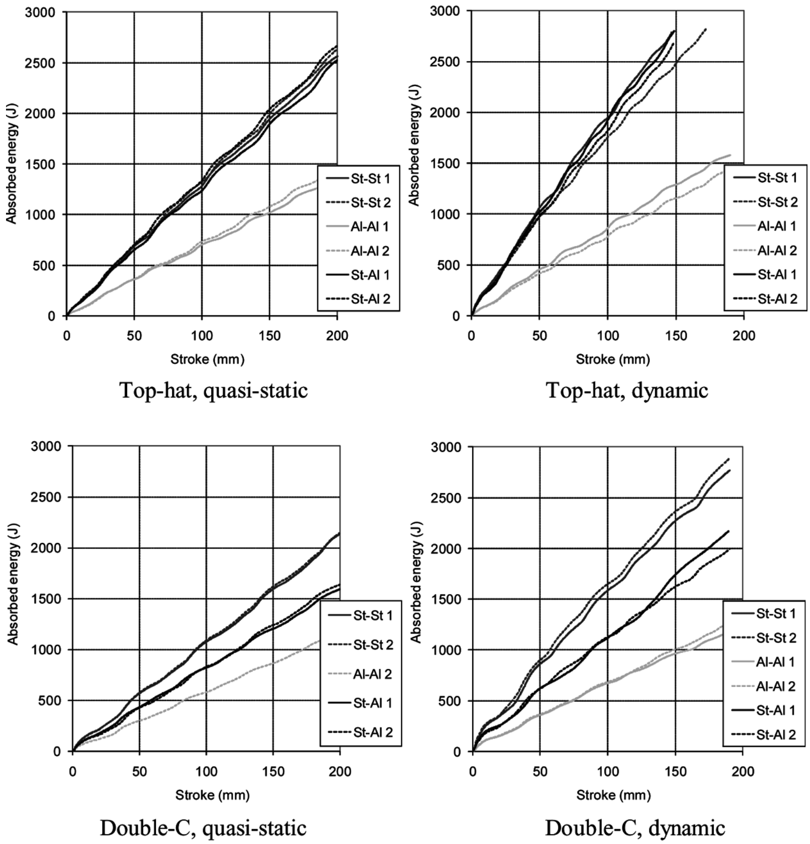

FIGURE 13 Absorbed energy-stroke curves from the examined components.

aluminium plate, the differences in terms of energy absorption and dissipation are negligible. This is also shown in Table 3. In the case of the double-C columns, the energy absorption of the hybrid solution is an average of the other two options with similar materials.

However, the purely aluminium components, and the hybrid ones, are lighter, and this brings an advantage in terms of specific energy absorption. This is reported in Table 3, last column on the right. From this perspective, for the double-C section columns, the performance is quite similar in all cases. Instead, for top-hat section columns, the performance of the aluminium columns is better than the steel ones, and even better are the hybrid solutions of a steel hat with an aluminium plate. This is justified by the observation (see Fig. 6 and 8 and Reference [12]) that the more flexible plate tends to favour a more stable formation of the folds, with more energy absorption. This

TABLE 3 Energy Absorption Comparison

Case	Combination	Average load, P_m (kN)	Mass, m (g)	Specific average load, P_{ms} (N/g)
Top-hat static	St-St	12.9	405.0	31.8
	St-Al	12.8	290.0	44.1
	Al-Al	7.0	175.0	39.9
Top-hat dynamic	St-St	17.4	405.0	42.9
	St-Al	18.2	290.0	62.6
	Al-Al	8.0	175.0	45.5
Double-C Static	St-St	10.5	405.0	25.9
	St-Al	8.0	290.0	27.7
	Al-Al	5.9	175.0	33.6
Double- C dynamic	St-St	14.5	405.0	35.9
	St-Al	10.7	290.0	36.9
	Al-Al	6.3	175.0	35.8

cannot happen in the double-C components due to the intrinsic symmetry. In this case, the aluminium solution is still the better, apart from economic considerations.

5. NUMERICAL RESULTS

The numerical simulations were developed by means of the finite element solver LS-Dyna v9.71 [30], using the implicit formulation. In particular, only the hybrid solutions, aluminium bonded to steel, of the two geometries were simulated. The average size of the elements was 4 mm, a value that can be considered typical for the automotive crash applications: with a more refined mesh, using a smaller average elements size, it is possible to obtain more accurate results but this would be incompatible with the requirements of the finite element model of a complete car because the solution time would be too high. More details about this topic are given in [31]. For what concerns the material models, for both aluminium and steel, the *MAT_POWERLAW_PLASTICITY was used. This is a general purpose plastic material formulation, including both isotropic and kinematic options, for which the stress-strain curve can be inserted by means of a power law function. The material parameters were obtained from experimental results performed in the past by the present authors. For what concerns the adhesive, it was modelled by using the cohesive element formulation. The *MAT_COHESIVE_MIXED_MODE material card was used. For this material it is required to define at least six parameters: the stiffness of the adhesive layer, the failure force, and the toughness [32] along the normal and tangential directions [30]. These parameters were obtained from a series of experimental tests, single lap and peeling,

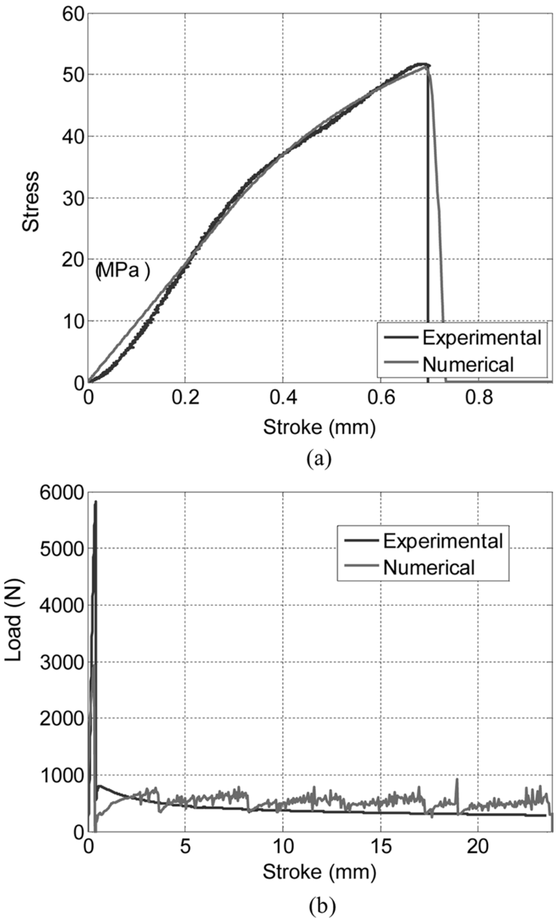

FIGURE 14 Results from the simulation of the (a) single-lap shear test and (b) peeling load test in comparison with the experimental data for the adhesive used.

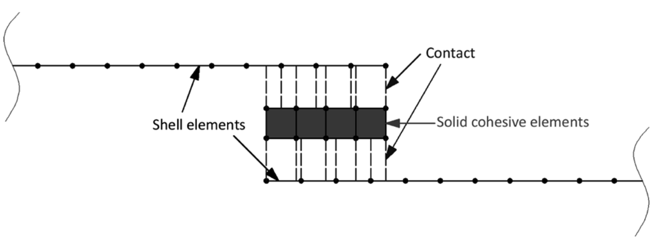

FIGURE 15 Description of the model of the adhesive joints used in the numerical simulations.

typically used to characterize the adhesive joint. The tests were then simulated to obtain the model parameters (a comparison of the numerical results with the experimental data is reported in Fig. 14).

The adhesive joint was simulated as follows: the shell elements used to simulate the metal sheet were positioned on their middle layer; the adhesive was modelled with a single layer of solid cohesive elements with transverse size equal to the adhesive thickness; and finally, the connection between the metal sheet shells and the

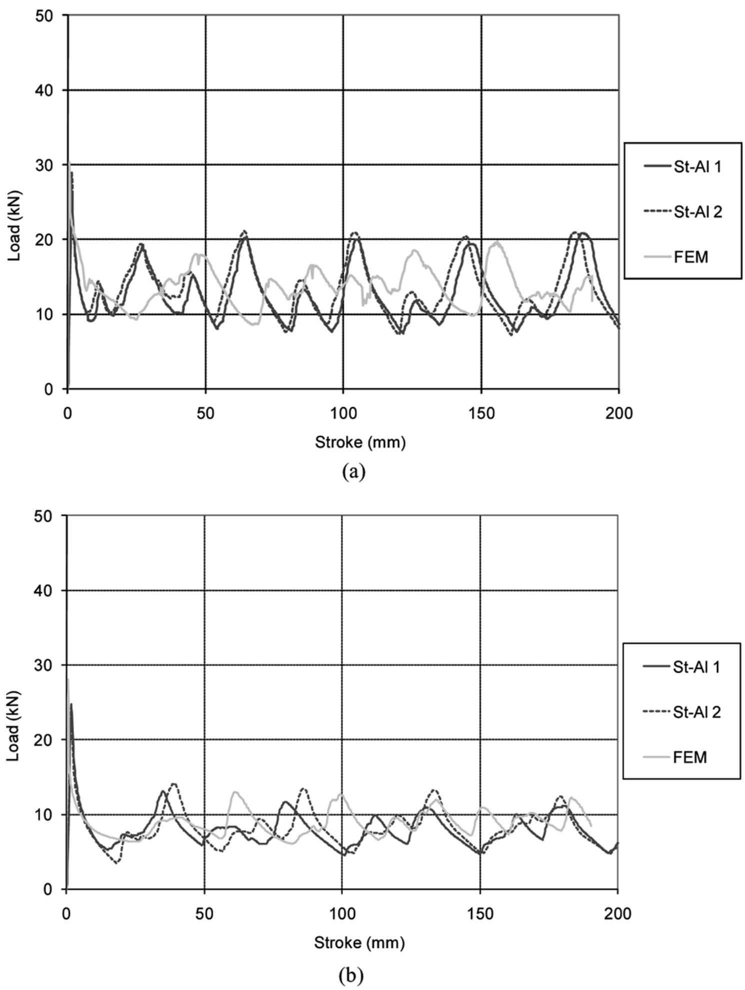

FIGURE 16 Quasi-static load-stroke curves obtained from (a) the top-hat section and (b) the double-C section.

adhesive solids was not done directly node by node, but a link was created using contact constraints—in particular, the *CONTACT_TIED card was used. Figure 15 explains the model in detail.

Only the quasi-static tests were simulated and good results were obtained, as can be seen in the following Figs. 16 and 17, both in terms of global behaviour and energy absorption.

5.1. Quasi-Static Simulations

The results of the quasi-static simulations are shown in Fig. 16. The two sections, top-hat and double-C, are compared there. The numerical result is shown compared with the experimental tests. In both cases there is a good correlation between experiments and simulations. In terms of absorbed energy the average load is overestimated by 6.8% with respect to the average experimental value obtained from the top-hat sections, and 9.8% for the double-C.

Figure 17 shows some snapshots of the columns during collapse. The comparison with the pictures taken during the experimental tests and shown in Figs. 6 and 10 is quite good, especially for the top-hat section. The shape of the folds, fold length, and final shape are reproduced with great fidelity.

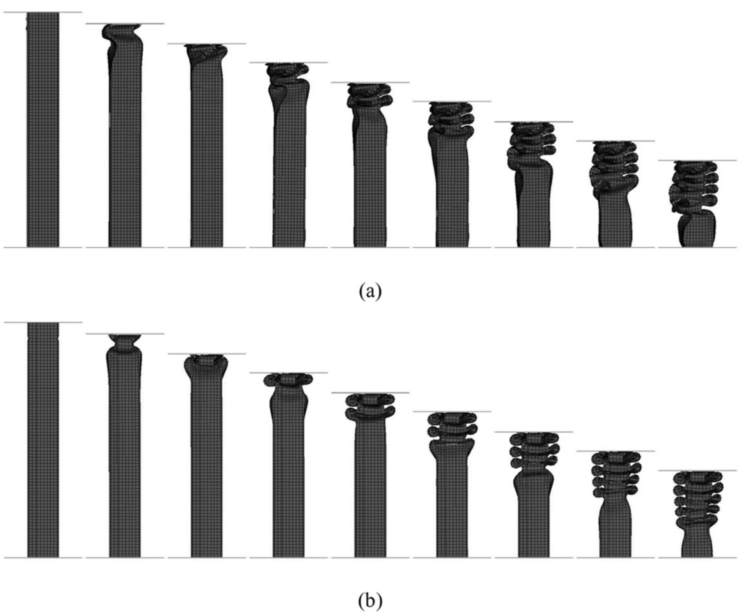

(a)

(b)

FIGURE 17 Simulation of the quasi-static progressive collapse of the (a) top-hat section columns and (b) double-C section columns.

6. CONCLUSIONS

Lightweight automotive structures are a necessity for the future development of less polluting and safer vehicles. A possible way to achieve this goal is to use lightweight materials, such as aluminium, sometimes coupled with more conventional materials such as steels. Joining different materials can be a problem with spot-welding, often even impossible. In this work, adhesively bonded hybrid structures, crash boxes, of aluminium and steel, have been studied. The performance is evaluated in terms of energy absorption in a stable axial plastic progressive collapse. This is the way crash boxes, thin-walled prismatic columns, are used in the front of most vehicles.

It was shown that a traditional top-hat shaped crash box, in the hybrid configuration of an aluminium plate bonded to a steel hat section, has the same efficiency as a whole steel structure. The hybrid structure is even better taking into account the lower weight. The hybrid double-C structure, instead, does not exhibit a better performance, and it is rather intermediate.

Simulations of the collapse in quasi-static tests have been shown: the correlation between the experiments and the simulations is very good when the right material parameters and models are set and chosen.

ACKNOWLEDGMENTS

The support of Henkel Loctite, in the person of Mr. Piero Mauri, is gratefully acknowledged for the realization of this work.

REFERENCES

[1] Davies, G., *Materials for Automobile Bodies*, (Elsevier, Oxford, 2003).
[2] Belingardi, G. and Avalle, M., *Mobility Vehicle Mechanics* **30** (2–3), 51–65 (2004).
[3] Schönfeld, R., Proceedings of the Workshop on Structural Adhesives (Politecnico di Torino, Vercelli, 2006). On-line: http://www.univer.polito.it/adesivi_download/26_lunedi/sessione2/Schoenfeld/Crash%20Resistant%20Structural%20Bonding.pdf.
[4] Avalle, M., *Proceedings of the 12th International Conference on Experimental Mechanics (ICEM12): Advances in Experimental Mechanics*, (McGraw-Hill, Bari, 2004), Paper No. 253.
[5] Fay, P. A. and Suthurst, G. D., *Int. J. Adhes. Adhes.* **10** (3), 128–138 (1990).
[6] Avalle, M., Belingardi, G., and Vadori, R., *Proceedings of the XXX National Conference of the Italian Association for Stress Analysis (AIAS)*, (Alghero, Italy 2001), Paper No. 016.
[7] Rivett, R. M., Riches, S. T., and Westgate, S. A., *Sheet Metal Welding Conference III*, (Southfield, MI, USA, 1988), American Welding Soc. Paper No. 5, pp. 1–35.
[8] Radlmayr, K.-M., Ponschab, H., Stiaszny, P., and Till, E., Proceedings of the 26th ISATA Conference on Road and Vehicle Safety, (Aachen, Germany, 1993), Paper 93SF061.

[9] Geoffroy, J. L., Cambien, I., and Jouet, A., *La metallurgia Italiana* **85** (6), 377–382 (1993).
[10] Bastawros, A. F., Proceedings of the International Body Engineering Conference (IBEC) on Interior, Safety and Environment, (Warren, MI, USA, 1997), pp. 98–104.
[11] Belingardi, G., Goglio, L., and Rossetto, M., *Int. J. Adhes. Adhes.* **25**, 173–180 (2002).
[12] Peroni, L., Avalle, M., and Belingardi, G., *Int. J. Impact Eng.* **36**, 498–511 (2009).
[13] Jones, N., *Structural Impact*, (Cambridge University Press, New York, 1997).
[14] Thornton, P. H., Mahmood, H. F., and Magee, C. L., *Structural Crashworthiness*, (Butterworths, Oxford, UK, 1983), pp. 96–117.
[15] Wierzbicki, T. and Abramowicz, W., *Structural Failure*, (John Wiley, New York, 1989), pp. 281–329.
[16] Johnson, W. and Reid, S. R., *Appl. Mech. Rev.* **31** (3), 277–288 (1978). Update: Steele, C. R., ed., *Appl. Mech. Rev.* **39**, 303–319 (1986).
[17] Abramowicz, W. and Jones, N., *Int. J. Impact Eng.* **4** (4), 243–270 (1986).
[18] White, M. D. and Jones, N., *Int. J. Mech. Sci.* **41**, 179–208 (1999).
[19] White, M. D. and Jones, N., *P. I. Mech. Eng. D-J. Aut.* **213** (3), 259–278 (1999).
[20] Alexander, J. M., *Q. J. Mech. Appl. Math.* **13** (1), 10–15 (1960).
[21] Wierzbicki, T. and Abramowicz, W., *J. Appl. Mech.* **50** (4), 727–734 (1983).
[22] Abramowicz, W. and Wierzbicki, T., *J. Appl. Mech.* **56** (3), 113–120 (1989).
[23] White, M. D., Jones, N., and Abramowicz, W., *Int. J. Mech. Sci.* **41**, 209–233 (1999).
[24] White, M. D. and Jones, N., *P. I. Mech. Eng. D-J. Aut.* **213** (4), 307–325 (1999).
[25] Schneider, F. and Jones, N., *P. I. Mech. Eng. D-J. Aut.* **218** (2), 131–158 (2004).
[26] Belingardi, G., Avalle, M., Fizzotti, R., and Tarditi, A., *Proceedings ATA (Associazione Tecnica dell'Automobile) Conference 2001*, (Florence, Italy, 2001), Paper 01A1043.
[27] Peroni, L. and Avalle, M., Experimental investigation of the energy absorption capability of bonded crash boxes in: *Structures Under Shock and Impact IX*, (WIT Press, Ashurst, UK, 2006), pp. 445–454.
[28] Grant, L. D. R., Adams, R. D., and da Silva, L. F. M., *Int. J. Adhes. Adhes.* **29**, 405–413 (2009).
[29] Grant, L. D. R., Adams, R. D., and da Silva, L. F. M., *Int. J. Adhes. Adhes.* **29**, 535–542 (2009).
[30] LSTC, LS-DYNA. Keyword User's Manual, Version 971 (LSTC, Livermore, 2007).
[31] Peroni, L., Martella, M., and Gastaldin, D., *Proceedings of the VII International Conference on Computational Plasticity*, (CIMNE, Barcelona, Spain, 2003).
[32] Pirondi, A., Fersini, D., Perotti, E., and Moroni, F., *Proceedings of the IGF National Conference*, (Milano, Italy, 2007), pp. 85–94. (Grafiche GSS, Arzago, d'Adda, BG, Italy)